Photoexcitation dynamics in an alternating polyfluorene copolymer

M. Westerling, H. Aarnio, R. Österbacka, and H. Stubb
Department of Physics, Åbo Akademi University, Porthansgatan 3, FIN-20500 Turku, Finland

S. M. King and A. P. Monkman
Department of Physics, University of Durham, DH1 3LE Durham, England, United Kingdom

M. R. Andersson
Department of Organic Chemistry and Polymer Technology, Chalmers University of Technology, Kemivägen 4, S-41296 Göteborg, Sweden

K. Jespersen, T. Kesti, A. Yartsev, and V. Sundström
Department of Chemical Physics, Lund University, P.O. Box 124, SE-22100 Lund, Sweden
(Received 22 December 2006; revised manuscript received 4 April 2007; published 29 June 2007)

We have used transient photoinduced absorption on femtosecond to nanosecond time scales as well as delayed fluorescence up to microseconds to study the photogeneration and recombination of charges in thin films of the alternating polyfluorene copolymer poly[2,7-(9,9-dioctylfluorene)-*alt*-5,5-(4′,7′-di-2-thienyl-2′,1′,3′-benzothiadiazole)]. We interpret the results using a coupled rate equation model and find that we can fit all our experimental results with a single set of parameters. The model includes prompt (<0.1 ps) as well as slower (~0.1–1 ns) charge-pair formation, which we attribute to Coulombically bound intra- and interchain polaron pairs, respectively. The intrachain polaron pairs are promptly generated from vibronically excited (hot) primary singlet excitons S_1^* and recombine geminately back to the lowest singlet exciton state S_1 with a lifetime distribution having a mean lifetime of ~2.4 ps. The interchain polaron pairs, which can be seen as precursors to free charges, are formed via two channels: via singlet excitons being dissociated with a linear rate constant of ~5 ns as well as via a time-dependent bimolecular exciton-exciton annihilation process generating higher-energy exciton states S_n^* of which a fraction subsequently dissociates into interchain polaron pairs. We observe a total yield of 12%–23% interchain polaron pairs (a precursor to free polarons), depending on the excitation intensity used. This also defines the upper limit of the free polaron yield at zero electric field in this material. The long-lived interchain polaron pairs recombine geminately back to the ground state or to singlet excitons with a broad distribution of lifetimes having a mean lifetime of ~0.27 μs. The fraction of interchain polaron pairs recombining back to singlet excitons, with subsequent radiative decay back to the ground state, gives rise to delayed fluorescence extending to microsecond time scales.

DOI: 10.1103/PhysRevB.75.224306 PACS number(s): 78.66.Qn, 71.20.Rv, 73.50.Gr

I. INTRODUCTION

Poly(9,9-dioctylfluorene) (PFO) and related polyfluorene derivatives have recently emerged as a promising class of conjugated polymers for optoelectronic applications such as light-emitting diodes,[1] photodiodes, and solar cells. Due to their high luminescence efficiency, good charge-transport characteristics,[2] thermal stability,[3] and tunability of physical parameters through chemical modification or copolymerization, these conjugated polymers have become commercially interesting. Especially alternating polyfluorene copolymers, with extended absorption in the red part of the visible spectrum, have shown to be good candidates for organic solar cells. One such copolymer is the novel low-band-gap copolymer poly[2,7-(9,9-dioctylfluorene)-*alt*-5,5-(4′,7′-di-2-thienyl-2′,1′,3′-benzothiadiazole)] (APFO3), which has a built-in charge-transfer character by design.[4] Bulk heterojunction solar cells made from blends of APFO3 and the soluble fullerene derivative [6,6]-phenyl-C_{61}-butyric acid methyl ester (PCBM) have shown a power conversion efficiency of up to 2.8%.[5,6] In order to further improve and develop these applications, it is of utmost importance to understand the photophysics and especially the charge-carrier photogeneration and recombination mechanisms in these materials. This has, to some degree, been studied before by Zhang *et al.*[6] and Jespersen *et al.*[7] Zhang *et al.* focus mainly on the influence of solvent mixing on the performance of APFO3:PCBM solar cells and show, using transient absorption spectroscopy that adding a small amount of chlorobenzene to a chloroform solution improves the charge generation efficiency. Jespersen *et al.*, on the other hand, use time-resolved spectroscopy to study charge generation efficiency as a function of PCBM concentration in APFO3:PCBM solar cells and compare the results with the measured short circuit current. Neither of these articles focus on the neat APFO3 polymer (although some results are shown), which, due to its built-in charge-transfer character, is different from most polymers commonly used for solar cell applications, and would therefore warrant an in-depth study of its own. Also, no attempt has so far been made to model the photoexcitation dynamics as a whole in this polymer. Thus, in this paper, we focus on studying and modeling in detail the formation and recombination of photoexcitations in neat APFO3.

There are basically two main descriptions of charge-carrier (polaron) photogeneration in pristine conjugated polymers. The first view assumes direct photogeneration of

free polarons via optical interband transitions,[8,9] whereas the second view considers charge-carrier generation as a two-step process, in which neutral singlet excitons are the primary photoexcitations created by photon absorption, followed by exciton dissociation into Coulombically bound intra- and/or interchain polaron pairs.[10–15] Polaron pairs can subsequently either recombine or fully separate into free polarons. Although most of the studies in the literature support the latter view, the mechanisms governing the singlet exciton dissociation into polaron pairs as well as their subsequent recombination dynamics are poorly understood.

In this paper, we report femtosecond to nanosecond transient photoinduced absorption (PA) as well as microsecond delayed fluorescence (DF) to study the photogeneration and recombination of charges in thin films of pristine APFO3. Using a long delay line, the PA was measured from 100 fs to 10 ns, i.e., over five orders of magnitude in time, giving us a unique possibility of studying the generation as well as the recombination of charges and their interplay with singlet excitons in APFO3. From the PA and DF (1 ns–100 μs) data, together with numerical fits to a rate equation model, we suggest that (geminate) Coulombically bound intrachain polaron pairs (PP_1), hereafter referred to as simply intrachain polaron pairs, are created from primary vibronically excited (hot) singlet excitons S_1^*, with a yield of 30%, on time scales shorter than 0.1 ps. The intrachain polaron pairs subsequently recombine dispersively within ~2.4 ps to the lowest singlet exciton state S_1.

Furthermore, our data suggest that interchain polaron (PP_2) pairs are formed via two different processes, as has previously been observed in methyl-substituted ladder-type poly(*para*-phenylene).[16] The first process which dominates at low pump intensities is linear and attributed to singlet exciton dissociation (at defects or dissociation sites) with a rate constant of ~5 ns, whereas the second process which dominates at moderate to high pump intensities is nonlinear (quadratic) and attributed to a two-step exciton-exciton annihilation process generating higher-energy exciton states S_n^*, of which a fraction subsequently dissociates into interchain polaron pairs. The interchain polaron pairs are long lived, and we suggest that they geminately recombine back to the ground state or to singlet excitons with a broad distribution of lifetimes (mean lifetime of ~0.27 μs). We also interpret the observed DF as originating from the fraction of interchain polaron pairs recombining back to singlet excitons, with subsequent radiative decay back to the ground state.[11,17] We would like to point out that this model applies to APFO3 and closely related materials, but that it due to APFO3:s built-in charge-transfer character should not necessarily be taken as a general model for neat polymers.

II. EXPERIMENT

APFO3 was synthesized as described by Svensson *et al.*[4] The APFO3 film used in the PA measurements was made by spin casting from a 15 mg/ml chloroform solution on a sapphire substrate. The thickness of the film was measured with an atomic force microscope (Park Scientific Instruments, Autoprobe CP) to be 135 nm. The absorption and photoluminescence spectra (PL) of the film were measured using a spectrophotometer (Hitachi, U-3200) and a luminescence spectrometer (Perkin Elmer, LS50B), respectively. The sample was placed inside a continuous gas flow cryostat (Oxford, Optistat^{DN}), which kept the temperature of the sample between 80 and 300 K. Transient PA was measured using an ultrafast pump-probe setup. The measurement system was based on a Ti:sapphire laser (Clark-MXR, CPA-2001), from which excitation and probe pulses were generated by noncollinear optical parametric amplifiers. The pulse width was ~50 fs, and the probe light was measured using Si photodiodes. A long delay line for the probe pulse allowed for straightforward measurements in the 100 fs–10 ns time interval. The pump-probe setup has been described in more detail elsewhere.[18]

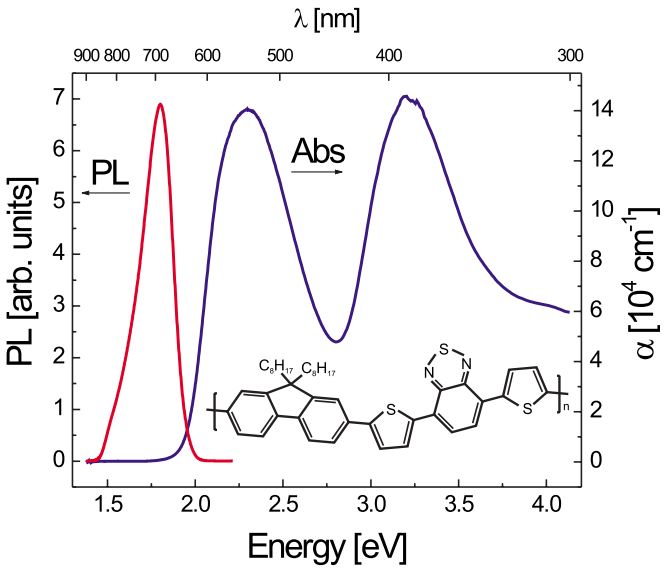

FIG. 1. (Color online) Absorption and PL spectra of APFO3 at 293 K [excitation wavelength λ_{exc}=543 nm (2.29 eV)]. The chemical structure of APFO3 is shown as an inset.

For the DF measurements, an APFO3 sample was prepared by spin casting from a 20 mg/ml chloroform solution on a round sapphire substrate. An yttrium aluminum garnet laser at 355 nm was used to excite the sample, which was kept at 80 K, and the resulting luminescence was measured using a spectrograph and a gated, intensified charge coupled device (CCD) detection system. Time-dependent luminescence was measured by varying the delay between excitation and collection of light and by varying the gate width (integrating time) for the CCD. In this way, luminescence could be measured over many orders of magnitude in both time and signal strength. This method has been previously discussed elsewhere.[19,20]

III. RESULTS AND DISCUSSION

A. Photoinduced absorption

The absorption and PL spectra as well as the chemical structure of APFO3 are shown in Fig. 1. The absorption shows an onset at roughly 2 eV (620 nm) and has two dis-

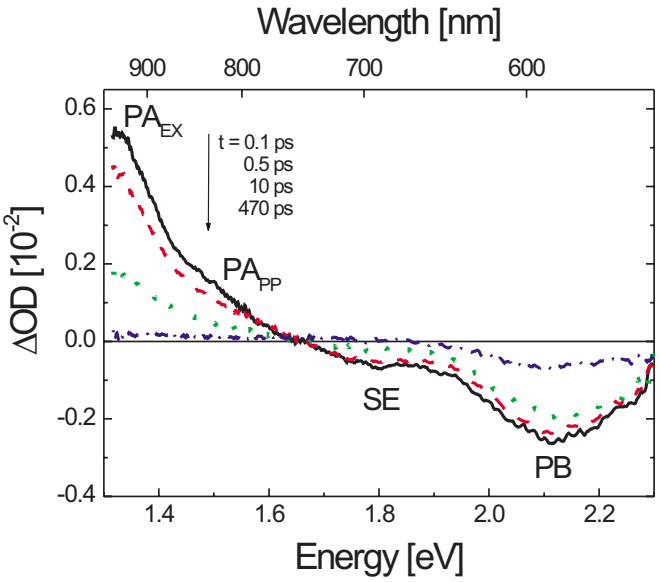

FIG. 2. (Color online) Transient PA spectra of APFO3 at 293 K for different time delays between pump and probe: 0.1 ps (solid line), 0.5 ps (dashed line), 10 ps (dotted line), and 470 ps (dash-dotted line). The pump wavelength and pulse duration are given by $\lambda_{pump}=570$ nm (2.18 eV) and $\Delta t_{pump}\sim 140$ fs, respectively.

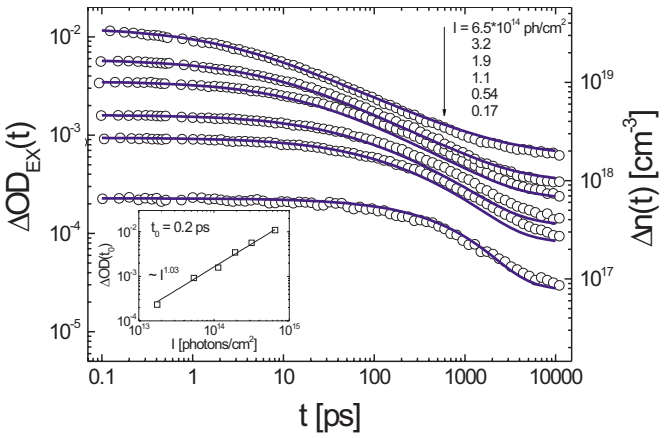

FIG. 3. (Color online) Transient PA dynamics of the PA_{EX} band at 1.27 eV (975 nm) in APFO3 for different pump intensities, measured at $T=80$ K using the pump wavelength $\lambda_{pump}=570$ nm (2.18 eV). The solid lines are numerical fits to the rate equation model presented in Sec. IV. The photoexcitation concentration $\Delta n(t)$ on the y axis to the right is directly related to $\Delta\mathrm{OD}(t)$ via the relation $\Delta n(t)=[(\ln 10)\alpha_L/\sigma]\times\Delta\mathrm{OD}(t)$, where $\alpha_L(570\ \mathrm{nm})=1.26\times10^5\ \mathrm{cm}^{-1}$ and $\sigma=10^{-16}\mathrm{cm}^2$ (see Sec. IV). The pump intensity dependence of the PA_{EX} band taken at $t=0.2$ ps is shown in the inset, and the solid line is a fit to $PA_{EX}\sim I^{\delta}$, yielding $\delta\approx1.03$.

tinct featureless absorption bands at 2.30 eV (540 nm) and 3.22 eV (385 nm), respectively. APFO3 was designed to have a degree of internal charge-transfer character, and the 2.30 eV band has previously been assigned to the $S_0\rightarrow S_1$ transition with the electron residing on the benzothiadiazole unit and the hole delocalized over the fluorene and thiophene units, whereas the 3.22 eV band is identified with a delocalized $\pi\rightarrow\pi^*$ transition.[21,22] The PL peaks at 1.8 eV (689 nm) and no vibronic structures are seen at room temperature.

The transient PA spectrum in the spectral region from 1.32 to 2.30 eV (540–940 nm), measured under annihilating conditions, is shown for different delay times in Fig. 2. The negative PA band at ~2.1 eV, present at all delay times, overlaps with the spectral position of the ground-state absorption and is therefore attributed to photoinduced bleaching (PB) of the $S_0\rightarrow S_1$ transition. The smaller negative band at ~1.8 eV, which is present at early times (0.1–10 ps), appears at the same spectral position as the PL (where there is no ground-state absorption) and is thus mainly attributed to probe-induced stimulated emission (SE) of singlet excitons ($S_1\rightarrow S_0$). The region from 1.32 to 1.65 eV (752–940 nm) shows a positive PA band in which two spectral features can be distinguished, a smaller (amplitude) band labeled PA_{PP} extending from 1.43 to 1.65 eV (752–865 nm) and a larger (amplitude) band labeled PA_{EX} rising up below 1.43 eV (>865 nm). In closely related polyfluorene materials as well as other conjugated polymers, the PA_{EX} band has been attributed to excited-state absorption, i.e., the $S_1\rightarrow S_n$ transition of the lowest singlet exciton to a higher-lying exciton state, whereas the PA_{PP} band has been attributed to polaron and/or polaron pair absorption.[23–26] Furthermore, continuous-wave photomodulation measurements on APFO3 have shown that long-lived polarons have a broad absorption band extending from 1.2 to 1.9 eV,[27] in good agreement with the broad positive band extending from 1.32 to 1.9 eV in the 470 ps PA spectra in Fig. 2. Thus, in accordance with these previous studies, we assign the PA_{PP} band to mainly polaron pairs (see details below), and the PA_{EX} band to excited-state absorption plus a contribution from polaron pairs due to the broad underlying PA_{PP} band.

In order to study the dynamics of the photoexcitations associated with the PA_{EX} and PA_{PP} bands, we measured the transient PA decay as a function of pump intensity at 1.27 eV (975 nm) and 1.6 eV (775 nm), respectively. The results are shown in Figs. 3 and 4. From Fig. 3, we see that the decay of the PA_{EX} signal becomes faster when the pump intensity is increased, indicative of a second-order decay process being present already from the lowest pump intensities [$\sim1.7\times10^{13}$ photons/(cm^2 pulse)]. At the longest times (~10 ns), the decay in Fig. 3 levels out, indicating that there is some other longer-lived photoexcitation contributing to the PA_{EX} signal. Furthermore, the inset in Fig. 3 shows that the amplitude of the PA_{EX} signal taken at ~0.2 ps scales approximately linearly with the pump intensity. The linear pump intensity dependence is in good agreement with the assignment that PA_{EX} is mainly due to singlet excitons, since singlet excitons are assumed to be the primary photoexcitations in APFO3. Furthermore, it has been well documented that at sufficiently high initial excitation density, the decay rate of singlet excitons in conjugated polymers is enhanced due to bimolecular exciton-exciton annihilation (EEA).[24,28–31] EEA is a second-order process that occurs through energy transfer between polymer segments and leads to a higher-energy excited state S_n^*. Since we attribute the PA_{EX} to mainly singlet excitons, it is natural to interpret the intensity dependent decay in Fig. 3 as being due to EEA.

The decay dynamics of PA_{PP} seen in Fig. 4 clearly indicates that two different processes take place on two dif-

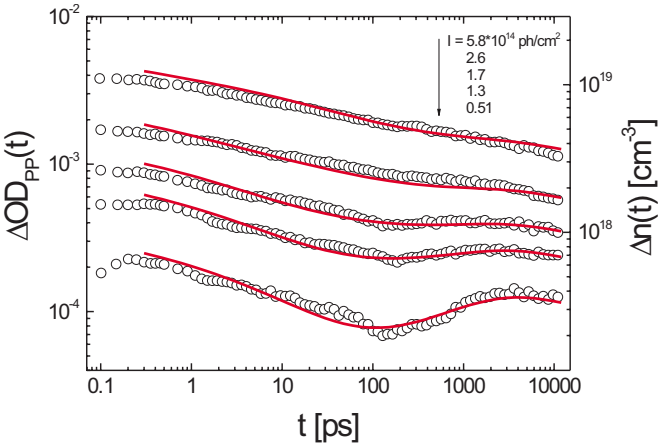

FIG. 4. (Color online) Transient PA dynamics of the PA_{PP} band at 1.6 eV (775 nm) in APFO3 for different pump intensities, measured at $T=80$ K using the pump wavelength $\lambda_{pump}=570$ nm (2.18 eV). The photoexcitation concentration $\Delta n(t)$ on the right y axis is directly related to $\Delta \mathrm{OD}(t)$ via the same relation as in Fig. 3. The solid lines are numerical fits to the rate equation model presented in Sec. IV.

ferent time scales. Initially, there is a fast decay on the time scale of ~10 ps followed by a slow buildup starting at ~100 ps. For the lowest pump intensity [~5.1×10^{13} photons/(cm^2 pulse)], the slow buildup reaches a maximum at ~3 ns and subsequently starts decaying on time scales larger than ~10 ns. For larger pump intensities, the slow buildup becomes less pronounced compared to the fast initial decay, and the maximum position shifts toward shorter times. The fast initial decay has been observed in other conjugated polymers and has previously been assigned to geminate recombination of intrachain polaron pairs.[25,32–34] Intrachain polaron pair photogeneration is considered as a two-step process in which neutral singlet excitons are the primary photoexcitations created by photon absorption, followed by exciton dissociation into intrachain polaron pairs. However, there are still two views regarding the need for higher-lying states in the exciton dissociation process. The first view assumes that photon absorption leads to the creation of vibrationally excited (hot) singlet excitons S_1^*, with subsequent dynamics occurring via two different pathways: (1) internal conversion of hot excitons into "cold" excitons ($S_1^*\rightarrow S_1$) and (2) a fraction of the hot excitons dissociate into intrachain polaron pairs on an ultrafast (~100 fs) time scale ($S_1^*\rightarrow \mathrm{PP}_1$). A theoretical model describing this on-chain ultrafast dissociation of unrelaxed excitons has been developed by Arkhipov *et al.*[35–37] Although we are using an excitation energy close to the optical gap of APFO3 and therefore do not provide much excess energy to the excitons, we still believe that this scenario could be feasible given the inherent charge-transfer character of APFO3. The second view assumes that photon absorption leads to the creation of singlet excitons S_1, of which a fraction at high excitation intensities subsequently absorbs a second pump photon during the pump pulse (sequential excitation), promoting them to a higher-energy exciton state S_n^*. The highly excited exciton states S_n^* then decay via two routes: (1) internal conversion back to singlet excitons ($S_n^*\rightarrow S_1$) and (2) dissociation into intrachain polaron pairs ($S_n^*\rightarrow \mathrm{PP}_1$). The first view predicts a linear pump dependence, whereas the second view predicts a quadratic pump intensity dependence of the PA_{PP} band at short time scales. Since the amplitude of the PA_{PP} band taken at 0.2 ps (not shown) scales approximately linearly with pump intensity, we conclude that the fast initial decay is due to recombination of intrachain polaron pairs which have been created from primary vibronically excited singlet excitons S_1^* on time scales shorter than 0.1 ps. It may be noted that linear pump intensity can also arise in the case of sequential excitation if the lowest singlet exciton population is saturated.[15,24] However, since the observed pump intensity dependence of the PA_{EX} band (inset in Fig. 3) is linear and no saturation is observed (for the used intensities), we have further support for the conclusion that sequential excitation is not the dominant mechanism for fast (subpicosecond) polaron pair generation in APFO3. This is in good agreement with the conclusions made by Stevens *et al.* in the closely related polyfluorene copolymer poly(9,9-dioctylfluorene-*co*-benzothiadiazole).[24] Since the intrachain polaron pairs are geminate in nature, it is likely that a fraction of them rapidly recombines geminately back to singlet excitons instead of recombining to the ground state, unless they are able to escape their mutual Coulomb potential and become free polarons. Thus, we mainly attribute the initial fast decay (~10 ps) of the PA_{PP} signal in Fig. 4 to geminate recombination of intrachain polaron pairs reforming singlet excitons. We note, however, that the SE band exhibits a redshift due to relaxation of vibronically excited singlet excitons on a time scale up to ~3 ps (not shown), which can distort the apparent dynamics of the PA_{PP} band at short times in case of spectral overlap. The overall behavior observed should still be that of the polaron pairs, as comparing the amplitudes of the measured PA transients above shows that we are not measuring as close to the SE band as it would seem from Fig. 2.

The slow buildup of the PA_{PP} signal (Fig. 4) beginning at ~100 ps clearly indicates the formation of a long-lived (lifetime longer than ~10 ns) photoexcitation. We observe that the formation of the long-lived photoproduct occurs on the same time scale as the decay of the PA_{EX} signal, suggesting that the photoproduct could be formed from singlet excitons. It is well known from literature that charge generation can take place following a two-step EEA process, in which higher-energy exciton states S_n^* are formed, of which a fraction subsequently dissociates into polaron pairs.[16] It has been suggested that the polaron pairs produced by EEA are mainly interchain polaron pairs, where the Coulombically bound charges reside on two adjacent polymer chains.[31] Moreover, it has also been observed that charge-pair formation can occur due to dissociation of vibrationally relaxed singlet excitons at special defect or dissociation sites (such as chain crossings, kinks, aggregates, etc.) during their entire lifetime even in the absence of an electric field.[38] These interchain polaron pairs are expected to absorb in the same wavelength region as intrachain polaron pairs, and their lifetime has been observed to extend to tens of microseconds.[39] These observations are in good agreement with the buildup and decay of the long-lived photoproduct observed in Fig. 4, and thus we

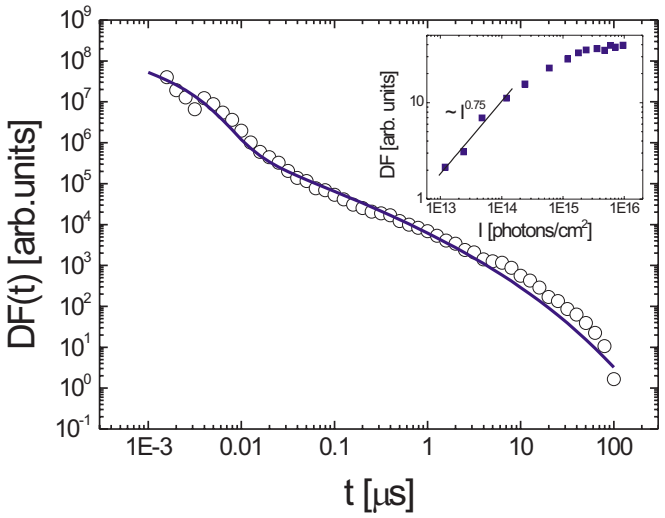

FIG. 5. (Color online) Time-resolved decay of the delayed fluorescence at 680 nm in APFO3. Measured at $T=80$ K using the excitation wavelength $\lambda_{exc}=355$ nm (3.50 eV). The excitation intensity dependence of the DF amplitude taken at 0.13 μs is shown in the inset. The solid line in the inset is a fit to DF$\sim I^{\epsilon}$, yielding $\epsilon \approx 0.75$.

attribute the photoproduct to interchain polaron pairs. Thus, we also expect the interchain polaron pairs to be formed both linearly (at low pump intensities) via dissociation at defect sites as well as nonlinearly (at high pump intensities) via bimolecular EEA. Based on this, we observe total interchain polaron pair yields ranging from 12% for the highest excitation intensity to 23% for the lowest excitation intensity. Because EEA reduces the number of singlet excitons, the yield is lower at high intensities.

At low to moderate concentrations, the long-lived interchain polaron pairs are expected to recombine (pairwise) with first-order kinetics back to the ground state or to singlet excitons. Due to the disorder in the positions and local orientations of the polymer chains, it is natural to assume that there is a Gaussian distribution of (polaron pair) intrapair distances and, therefore, also binding energies. Thus, one would expect a broad distribution of lifetimes, effectively showing up as time-dependent rate coefficients. Since a fraction of the interchain polaron pairs are expected to recombine back to singlet excitons, which can further recombine radiatively to the ground state, we should see delayed fluorescence (DF) displaying a broad distribution of lifetimes extending to microsecond time scales.

B. Delayed fluorescence

The time-resolved DF (1 ns–100 μs) measured at 1.82 eV (680 nm) is shown in Fig. 5. An excitation wavelength of 355 nm was used, but this should not affect the dynamics in any significant way compared to excitation at 570 nm, apart from an initial internal conversion from S_2 to S_1 with a decay time of 200 fs.[18] We have also measured some transient PA dynamics using 355 nm excitation (not shown) but cannot observe any significant differences compared to the results presented above. The observed DF consists of two components, a faster decay component on nanosecond time scales and a slower dispersive decay component extending to microsecond time scales. The excitation intensity dependence of the DF taken at 0.13 μs is shown in the inset of Fig. 5. At low to moderate excitation intensities, the DF scales sublinearly with intensity but saturates for intensities larger than 10^{15} photons/(cm^2 pulse). Time correlated single photon counting measurements performed on APFO3 in chloroform solution have shown that the fluorescence decay of singlet excitons is a single exponential decay with a lifetime of 3.25 ns.[18] In a film, this lifetime would be expected to be significantly shorter; we, however, observe a rather similar lifetime of 2 ns using our rate equation model. This lifetime is, however, in good agreement with the fast decay component observed in Fig. 5, and we therefore attribute the fast component to prompt fluorescence of singlet excitons.

DF in conjugated polymers is mainly interpreted as due to either bimolecular triplet-triplet annihilation[19,40,41] (TTA) or geminate recombination of Coulombically bound polaron pairs.[17,42–44] Rothe and Monkman argue that DF in ordinary conjugated polymers is always due to TTA.[45] APFO3, however, is designed to have an internal charge-transfer character, making it different from most conjugated polymers, and therefore we see it justified to also consider polaron pairs as a possible origin for our DF. In TTA, two long-lived triplet excitons annihilate in a bimolecular collisionlike process and give rise to a higher-energy singlet exciton state, which rapidly relaxes via internal conversion to the lowest singlet exciton state. The singlet exciton subsequently decays radiatively back to the ground state giving rise to DF. In the case of long-lived Coulombically bound polaron pairs, DF arises due to geminate charge recombination back to the singlet exciton (back transfer) and subsequent radiative decay to the ground state. If the slow DF component in Fig. 5 was due to TTA, one would expect a quadratic pump intensity dependence of the DF signal at low excitation intensities due to the bimolecular character of the TTA reaction, followed by a linear dependence at higher intensities (or sublinear, in case of dispersive triplet exciton migration).[17,19,45] Moreover, there should also be a clear temperature dependence of the DF decay, since the migration of triplet excitons is enhanced at higher temperatures, giving rise to enhanced TTA and thus a faster DF decay.[19] On the other hand, if the DF was due to recombination of long-lived polaron pairs, we would expect a linear or sublinear[17] pump intensity dependence. In this case, it has also been observed that the DF decay is relatively insensitive to the temperature.[17,44]

The measured intensity dependence of the DF in Fig. 5 is clearly sublinear at low intensities and saturates for high intensities. Thus, it cannot be seen as conclusive evidence for either polaron pairs or triplet excitons, but perhaps hints more toward polaron pairs as no superlinearity is observed at any of the intensities used. We also measured the temperature dependence of the DF decay. There is no temperature dependence in the range of 11–80 K, but at higher temperatures (120–280 K), the initial decay becomes slower and slower and then turns faster at a turning point that is moving toward shorter times with increasing temperature. This dependence is, however, quite weak and supports the polaron

pair picture more than the triplet exciton picture. Furthermore, we have been unable to observe any phosphorescence on wavelengths up to 1200 nm at 77 K. As polythiophenes have among the highest intersystem crossing rates of all polymers, we would expect to have some triplet excitons in APFO3 as well,[46] but the lack of observable phosphorescence means that potential triplet excitons either recombine nonradiatively or emit outside of our detection window. It could also indicate that we lack triplet excitons in APFO3 altogether; however, we do not have conclusive evidence to show this. Taken together, these observations suggest that DF in APFO3 is not due to TTA but more likely due to geminate recombination of long-lived polaron pairs. This is in good agreement with the earlier assignment of the long-lived photoproduct (observed in the PA decay in Fig. 4) to interchain polaron pairs, linking together the DF with the photoexcitations observed in PA. Although our results point more toward polaron pairs as the origin of DF, we cannot exclude the possibility of triplet excitons being present and possibly even contributing to the DF to some degree.

The observed DF decay Fig. 5 is not a single exponential decay but clearly shows a broad distribution of lifetimes, which is consistent with a broad distribution of polaron pair interpair distances as described earlier. A description of the DF decay resulting from dispersive geminate recombination of polaron pairs has been given by Nikitenko *et al.*[47] In this model, the charge carriers forming a polaron pair are assumed to undergo random walk (hopping) within their mutual Coulombic potential, the hopping sites being subject to a Gaussian distribution of energies. In the intermediate time regime this model predicts an algebraic (or power-law) type of decay, $\mathrm{DF}(t) \sim t^{-n}$ $(n \geqslant 1)$, with the exponent n increasing with increasing temperature. This can coarely explain the underlying reasons for our experimental observation, although the observed DF decay in Fig. 5 is not exactly of this form since the decay shows a clear downward curvature for all times. This kind of weak downward curvature in a log-log plot is better described by a phenomenological stretched exponential function of the form $\mathrm{DF}(t) \sim \exp(ct^{-m})$, where c and m $(0<m<1)$ are constants. This will be considered more in the next section when setting up the photophysical model describing both the PA and DF decays.

IV. PHOTOPHYSICAL MODELING AND ANALYSIS

In order to support the assignments made in the previous section, we have developed a simple rate equation model to simulate the PA and DF decays in Figs. 3–5. The basic assumptions of the model are as follows:

(1) Upon initial excitation by the laser, vibronically excited primary singlet excitons S_1^* are formed, of which a fraction f_{s_1} relaxes back to the lowest singlet exciton S_1 ($S_1^* \rightarrow S_1 + \text{phonons}$) and a fraction $(1-f_{s_1})$ dissociates into Coulombically bound intrachain polaron pairs PP_1 ($S_1^* \rightarrow \mathrm{PP}_1$), with both the relaxation and the dissociation taking place on ultrafast time scales <0.1 ps.

(2) Relaxed singlet excitons S_1 decay radiatively to the ground state with a rate constant k_{rad} ($S_1 \rightarrow S_0 + h\nu$) but also dissociate into interchain polaron pairs PP_2 (at defects, special dissociation sites, etc.) with a rate constant k_{spp2} ($S_1 \rightarrow \mathrm{PP}_2 + \text{phonons}$).

(3) At moderate to high pump intensities, singlet excitons S_1 undergo EEA according to $S_1 + S_1 \rightarrow S_0 + S_n^*$, generating higher-energy excitons S_n^*, of which a fraction subsequently relaxes back to S_1 and the rest dissociating into interchain polaron pairs PP_2. Hence, the net overall process is described in the model by a time-dependent bimolecular recombination rate of the form $(B_{ss}+B_{spp2})t^{\gamma_{ss}-1}$, where γ_{ss} is a constant $(0<\gamma_{ss}<1)$, the rate coefficient B_{SS} represents the fraction relaxing back to S_1, and the rate coefficient B_{spp2} represents the fraction dissociating into interchain polaron pairs. The power-law time dependence of the bimolecular rate coefficient is well known in conjugated polymers and arises from random walk (hopping) of singlet excitons in a landscape in which the energy of the hopping sites varies according to a Gaussian distribution.[48–50]

(4) The intrachain polaron pairs PP_1 recombine geminately back to singlet excitons S_1 ($\mathrm{PP}_1 \rightarrow S_1$) with a lifetime distribution represented by a simple first-order algebraic time-dependent rate of the form $A_{pp1s}t^{\alpha_{pp1s}-1}$, where A_{pp1s} and α_{pp1s} $(0<\alpha_{pp1s}<1)$ are constants. This form of rate leads to a stretched exponential decay $PP_1(t) \sim \exp(-(t/\tau_{pp_1})^{\alpha_{pp1s}})$ of the intrachain polaron pairs, with an overall lifetime of $\tau_{pp_1} = (\alpha_{pp1s}/A_{pp1s})^{1/\alpha_{pp1s}}$. Similar multiexponential kinetics has earlier been observed for intrachain polaron pairs in the polyfluorene PFO.[33]

(5) The interchain polaron pairs PP_2 are long lived and recombine geminately with a broad distribution of lifetimes extending to microseconds. A large fraction is expected to recombine nonradiatively to the ground state ($\mathrm{PP}_2 \rightarrow S_0 + \text{phonons}$), whereas a small fraction is assumed to dissociate into free polarons ($\mathrm{PP}_2 \rightarrow P^+ + P^-$) or recombine back to singlet excitons S_1 ($\mathrm{PP}_2 \rightarrow S_1$) resulting in DF. The lifetime and recombination of the free polarons have been studied before.[27] The overall process is described by a first-order time-dependent rate of the form $(A_{pp2s}+A_{pp20})t^{\alpha_{pp2s}-1}$, where the rate coefficient A_{pp2s} represents the "fraction" recombining to singlet excitons and the rate coefficient A_{pp20} represents the fraction recombining nonradiatively to the ground state or dissociating to free polarons. As earlier, α_{pp2s} is a constant $(0<\alpha_{pp2s}<1)$ describing the dispersivity of the decay, and an overall mean lifetime can again be defined as $\tau_{pp_2} = [\alpha_{pp2s}/(A_{pp2s}+A_{pp20})]^{1/\alpha_{pp2s}}$.

A schematic diagram of the formation and recombination channels for photoexcitations in APFO3 can be seen in Fig. 6, and the corresponding nonlinear coupled rate equations for the time evolution of the concentration of singlet excitons $S_1(t)$, intrachain polaron pairs $\mathrm{PP}_1(t)$, and interchain polaron pairs $\mathrm{PP}_2(t)$ are given by

$$\frac{dS_1}{dt} = -(k_{rad}+k_{spp2})S_1 - (B_{ss}+B_{spp2})t^{\gamma_{ss}-1}S_1^2 + A_{pp1s}t^{\alpha_{pp1s}-1}\mathrm{PP}_1 + A_{pp2s}t^{\alpha_{pp2s}-1}\mathrm{PP}_2, \quad (1a)$$

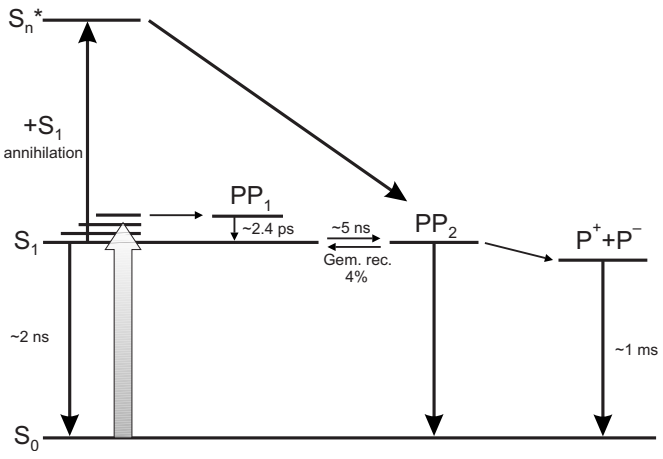

FIG. 6. Schematic diagram of the formation and recombination channels of photoexcitations in APFO3.

$$\frac{d\mathrm{PP}_2}{dt} = k_{spp2}S_1 + B_{spp2}t^{\gamma_{ss}-1}S_1^2 - (A_{pp2s} + A_{pp20})t^{\alpha_{pp2s}-1}\mathrm{PP}_2, \tag{1b}$$

$$\frac{d\mathrm{PP}_1}{dt} = -A_{pp1s}t^{\alpha_{pp1s}-1}\mathrm{PP}_1. \tag{1c}$$

Furthermore, the model assumes (as was assigned earlier) that the $\mathrm{PA}_{\mathrm{EX}}$ band at 1.27 eV is due to excited-state absorption from singlet excitons plus a contribution from polaron pairs (both intra- and interchain) and that the $\mathrm{PA}_{\mathrm{PP}}$ band at 1.6 eV is due to both intra- and interchain polaron pairs. This leads to the following two equations for the change in optical density (ΔOD) for the $\mathrm{PA}_{\mathrm{EX}}$ and $\mathrm{PA}_{\mathrm{PP}}$ bands:

$$\Delta\mathrm{OD}_{\mathrm{EX}}(t) = \epsilon_{s_1}S_1(t) + \epsilon_{pp1}\mathrm{PP}_1(t) + \epsilon_{pp2}\mathrm{PP}_2(t), \tag{2a}$$

$$\Delta\mathrm{OD}_{\mathrm{PP}}(t) = \epsilon_{pp1}\mathrm{PP}_1(t) + \epsilon_{pp2}\mathrm{PP}_2(t), \tag{2b}$$

where the coefficients ϵ_{s_1}, ϵ_{pp_1}, and ϵ_{pp_2} for an optically thick film ($\alpha_L d > 1$) are given by

$$\epsilon_{s_1} = \frac{\sigma_{s_1}}{(\ln 10)\alpha_L}, \quad \epsilon_{pp1} = \frac{\sigma_{pp1}}{(\ln 10)\alpha_L}, \quad \epsilon_{pp2} = \frac{\sigma_{pp2}}{(\ln 10)\alpha_L}. \tag{3}$$

Here, α_L is the absorption coefficient of the polymer at the pump wavelength, d is the thickness of the film, and σ_{s_1}, σ_{pp_1}, and σ_{pp_2} are the absorption cross sections for singlet excitons, intrachain polaron pairs, and interchain polaron pairs, respectively. In order to relate the decay of the DF to the equations above, we note that the DF is directly proportional to the radiative decay rate of singlet excitons, and thus we have

$$\mathrm{DF}(t) \sim \left(\frac{dS_1}{dt}\right)_{rad} \sim S_1(t). \tag{4}$$

The solid lines in Figs. 3–5 are simultaneous numerical fits (with the same set of parameters) using Eqs. (2a), (2b), and (4), [together with the rate equations (1a)–(1c)], respectively.

TABLE I. Summary of parameters used in modeling the recombination dynamics of APFO3.

Parameters	Value	Unit
k_{rad}	5.0×10^{8}	s^{-1}
k_{spp2}	2.0×10^{8}	s^{-1}
A_{pp1s}	200	$\mathrm{s}^{-\alpha_{pp1s}}$
A_{pp20}	26.7	$\mathrm{s}^{-\alpha_{pp2s}}$
A_{pp2s}	1.2	$\mathrm{s}^{-\alpha_{pp2s}}$
B_{ss}	1.6×10^{-13}	$\mathrm{cm}^3/\mathrm{s}^{\gamma_{ss}}$
B_{spp2}	2.1×10^{-14}	$\mathrm{cm}^3/\mathrm{s}^{\gamma_{ss}}$
α_{pp1s}	0.25	
α_{pp2s}	0.3	
γ_{ss}	0.6	

In the fits, we have used $\alpha_L(570\ \mathrm{nm}) = 1.26\times10^5\ \mathrm{cm}^{-1}$, and for simplicity, we have assumed that $\sigma_{s_1} = \sigma_{pp_1} = \sigma_{pp_2} = 10^{-16}\ \mathrm{cm}^2$. The overall agreement between the data and the simulated fits is relatively good considering that we are using a single set of parameters and the decays span over many orders of magnitude in time and pump intensity.

A summary of the parameters used in fitting the PA and DF decays is shown in Table I. Using these parameters, we have also separately plotted (in Fig. 7) the explicit time-dependence of the time dependent first- and second-order rates used in the rate equation model. Furthermore, overall mean lifetimes $\tau_{pp_1} = 2.4$ ps and $\tau_{pp_2} = 0.27\ \mu$s are obtained for the intra- and interchain polaron pairs, respectively (see definition of lifetimes above). From the amplitude of the DL decay curve, we can also estimate that ~4% of PP_{inter} undergo back transfer to S_1.

In earlier studies on the same material, we measured a polaron lifetime of ~1 ms, but we also observed another excitation that we assigned to polaron pairs and that recombined in a nondispersive way with a lifetime of ~20 μs.[27] In the model presented in this paper, the interchain polaron pairs are strongly dispersive with a shorter average lifetime of ~0.27 μs. One possible explanation for this discrepancy might be the existence of a lower limit in the lifetime distribution of the interchain polaron pairs. Thus, at long times,

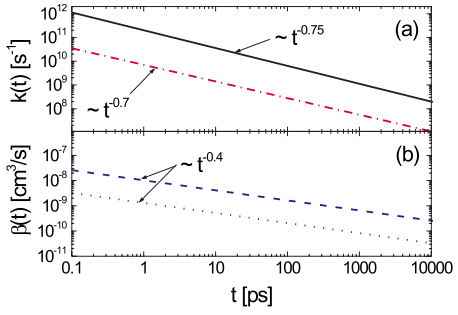

FIG. 7. (Color online) (a) Time dependence of first-order rate coefficients $k_{pp1s}(t) = A_{pp1s}t^{\alpha_{pp1s}-1}$ (solid line) and $k_{pp2s}(t) = (A_{pp2s} + A_{pp20})t^{\alpha_{pp2s}-1}$ (dash-dotted line). (b) Time dependence of second-order rate coefficients $\beta_{ss}(t) = B_{ss}t^{\gamma_{ss}-1}$ (dashed) and $\beta_{spp2} = B_{spp2}t^{\gamma_{ss}-1}$ (dotted).

we would only be left with the longest lifetime in the distribution and would therefore observe a nondispersive recombination. In the decay curve of the DF in Fig. 5, we observe a strong change in the decay dynamics at just below 100 μs, possibly indicating an end of the lifetime distribution. A similar behavior was observed at various temperatures for all curves measured (not shown). Fitting the end of the decay (20–100 μs) using a single exponential indeed reveals a lifetime of 21.6 μs.

It should be noted that our model is not intended to be a complete representation of all processes involved but rather a "simplest possible" approach for explaining our experimental results. Even though lots of effort have been put in optimizing the model and the parameters used, and we noticed no unnecessary degrees of freedom, there may be other processes and parameters that can explain our data equally well or even better.

V. CONCLUSION

In this work, we have used femtosecond to nanosecond transient photoinduced absorption as well as time-resolved delayed fluorescence to study the photogeneration and recombination of excitons and charges in thin films of pristine APFO3. We present a rate equation model, with which we have fitted all our experimental results simultaneously using a single set of parameters. From the PA and DF together with the rate equation model, we suggest that we have prompt ($<$0.1 ps) as well as slower charge-pair (0.1–1 ns) generation. The promptly generated charges are found to be intrachain polaron pairs, whereas the slowly generated charges are attributed to interchain polaron pairs. The intrachain polaron pairs are found to be short lived having a mean lifetime of $\sim$2.4 ps, in contrast to the interchain polaron pairs being long lived with an overall mean lifetime of $\sim$0.27 μs. The interchain polaron pairs are found to be generated from singlet excitons being dissociated with a linear constant of $\sim$5 ns, as well as via second-order exciton-exciton annihilation. The delayed fluorescence is found to originate from geminate recombination of long-lived interchain polaron pairs back to singlet excitons. We observe interchain polaron pair yields ranging from 12% for the highest excitation intensity to 23% for the lowest excitation intensity.

ACKNOWLEDGMENTS

Discussions with Olle Inganäs, Torbjörn Pascher, Swati De, and Manisankar Maiti are acknowledged. The studies in Lund were supported by the Center of Organic Electronics, funded by the Swedish Strategic Research Foundation (SSF). Support was also obtained from the Swedish Research Council, The Knut and Alice Wallenberg Foundation, and the Crafoord Foundation. Partial financial support was received from the Academy of Finland Project No. 107684, the Magnus Ehrnrooth Foundation, and the Integrated Initiative of Infrastructure project LASERLAB-EUROPE, Contract No. RII3-CT-2003-506350.

[1] A. W. Grice, D. D. C. Bradley, M. T. Bernius, M. Inbasekaran, W. W. Wu, and E. P. Woo, Appl. Phys. Lett. **73**, 629 (1998).
[2] M. Redecker, D. D. C. Bradley, M. Inbasekaran, W. W. Wu, and E. P. Woo, Adv. Mater. (Weinheim, Ger.) **11**, 241 (1999).
[3] M. Kreyenschmidt, G. Klaerner, T. Fuhrer, J. Ashenhurst, S. Karg, W. D. Chen, V. Y. Lee, J. C. Scott, and R. D. Miller, Macromolecules **31**, 1099 (1998).
[4] M. Svensson, F. Zhang, S. C. Veenstra, W. J. H. Verhees, J. C. Hummelen, J. M. Kroon, O. Inganäs, and M. R. Andersson, Adv. Mater. (Weinheim, Ger.) **15**, 988 (2003).
[5] O. Inganäs, M. Svensson, F. Zhang, A. Gadisa, N. K. Persson, X. Wang, and M. R. Andersson, Appl. Phys. A: Mater. Sci. Process. **79**, 31 (2004).
[6] F. Zhang, K. G. Jespersen, C. Björström, M. Svensson, M. R. Andersson, V. Sundström, K. Magnusson, E. Moons, A. Yartsev, and O. Inganäs, Adv. Funct. Mater. **16**, 667 (2006).
[7] K. G. Jespersen, F. Zhang, A. Gadisa, V. Sundström, A. Yartsev, and O. Inganäs, Org. Electron. **7**, 235 (2006).
[8] D. Moses, in *Primary Photoexcitations in Conjugated Polymers: Molecular Exciton versus Semiconductor Band Model*, edited by N. S. Sariciftci (World Scientific, Singapore, 1997).
[9] D. Moses, A. Dogariu, and A. J. Heeger, Phys. Rev. B **61**, 9373 (2000).
[10] M. Gailberger and H. Bässler, Phys. Rev. B **44**, 8643 (1991).
[11] E. L. Frankevich, A. A. Lymarev, I. Sokolik, F. E. Karasz, S. Blumstengel, R. H. Baughman, and H. H. Hörhold, Phys. Rev. B **46**, 9320 (1992).
[12] M. Yan, L. J. Rothberg, F. Papadimitrakopoulos, M. E. Galvin, and T. M. Miller, Phys. Rev. Lett. **72**, 1104 (1994).
[13] V. Dyakonov and E. Frankevich, Chem. Phys. **227**, 203 (1998).
[14] E. J. W. List, J. Partee, J. Shinar, U. Scherf, K. Müllen, E. Zojer, K. Petritsch, G. Leising, and W. Graupner, Phys. Rev. B **61**, 10807 (2000).
[15] C. Silva, A. S. Dhoot, D. M. Russell, M. A. Stevens, A. C. Arias, J. D. MacKenzie, N. C. Greenham, R. H. Friend, S. Setayesh, and K. Müllen, Phys. Rev. B **64**, 125211 (2001).
[16] D. Hertel, Yu. V. Romanovskii, B. Schweitzer, U. Scherf, and H. Bässler, Synth. Met. **116**, 139 (2001).
[17] Y. V. Romanovskii, A. Gerhard, B. Schweitzer, R. I. Personov, and H. Bässler, Chem. Phys. **249**, 29 (1999).
[18] K. G. Jespersen, A. Yartsev, T. Pascher, and V. Sundström, Synth. Met. **155**, 262 (2005).
[19] C. Rothe and A. P. Monkman, Phys. Rev. B **68**, 075208 (2003).
[20] S. King, C. Rothe, and A. P. Monkman, J. Chem. Phys. **121**, 10803 (2004).
[21] K. G. Jespersen, W. J. D. Beenken, Y. Zaushitsyn, A. Yartsev, M. Andersson, T. Pullerits, and V. Sundström, J. Chem. Phys. **121**, 12613 (2004).
[22] Q. Zhou, Q. Hou, L. Zheng, X. Deng, G. Yu, and Y. Cao, Appl. Phys. Lett. **84**, 1653 (2004).
[23] B. Kraabel, V. I. Klimov, R. Kohlman, S. Xu, H.-L. Wang, and D. W. McBranch, Phys. Rev. B **61**, 8501 (2000).

[24] M. A. Stevens, C. Silva, D. M. Russell, and R. H. Friend, Phys. Rev. B **63**, 165213 (2001).
[25] R. Pacios, J. Nelson, D. D. C. Bradley, T. Virgili, G. Lanzani, and C. J. Brabec, J. Phys.: Condens. Matter **16**, 8105 (2004).
[26] O. J. Korovyanko and Z. V. Vardeny, Chem. Phys. Lett. **356**, 361 (2002).
[27] H. Aarnio, M. Westerling, R. Österbacka, M. Svensson, M. R. Andersson, and H. Stubb, Chem. Phys. **321**, 127 (2006).
[28] M. Pope and C. E. Swenberg, *Electronic Processes in Organic Crystals and Polymers*, 2nd ed. (Oxford University Press, New York, 1999).
[29] Q.-H. Xu, D. Moses, and A. J. Heeger, Phys. Rev. B **68**, 174303 (2003).
[30] G. Dicker, M. P. de Haas, and L. D. A. Siebbeles, Phys. Rev. B **71**, 155204 (2005).
[31] I. B. Martini, A. D. Smith, and B. J. Schwartz, Phys. Rev. B **69**, 035204 (2004).
[32] J. G. Müller, U. Lemmer, J. Feldmann, and U. Scherf, Phys. Rev. Lett. **88**, 147401 (2002).
[33] T. Virgili, D. Marinotto, C. Manzoni, G. Cerullo, and G. Lanzani, Phys. Rev. Lett. **94**, 117402 (2005).
[34] L. Lüer, G. Cerullo, M. Zavelani-Rossi, and G. Lanzani, Chem. Phys. Lett. **381**, 751 (2003).
[35] V. I. Arkhipov, E. V. Emelianova, and H. Bässler, Phys. Rev. Lett. **82**, 1321 (1999).
[36] V. I. Arkhipov, E. V. Emelianova, S. Barth, and H. Bässler, Phys. Rev. B **61**, 8207 (2000).
[37] D. M. Basko and E. M. Conwell, Phys. Rev. B **66**, 155210 (2002).
[38] Y. Zaushitsyn, V. Gulbinas, D. Zigmantas, F. Zhang, O. Inganäs, V. Sundström, and A. Yartsev, Phys. Rev. B **70**, 075202 (2004).
[39] W. Graupner, J. Partee, J. Shinar, G. Leising, and U. Scherf, Phys. Rev. Lett. **77**, 2033 (1996).
[40] J. Partee, E. L. Frankevich, B. Uhlhorn, J. Shinar, Y. Ding, and T. J. Barton, Phys. Rev. Lett. **82**, 3673 (1999).
[41] S. A. Bagnich and A. V. Konash, Chem. Phys. **263**, 101 (2001).
[42] B. Schweitzer, V. I. Arkhipov, U. Scherf, and H. Bässler, Chem. Phys. Lett. **313**, 57 (1999).
[43] A. Hayer, H. Bässler, B. Falk, and S. Schrader, J. Phys. Chem. A **106**, 11045 (2002).
[44] C. M. Cuppoletti and L. J. Rothberg, Synth. Met. **139**, 867 (2003).
[45] C. Rothe and A. Monkman, J. Chem. Phys. **123**, 244904 (2005).
[46] H. D. Burrows, J. Seixas de Melo, C. Serpa, L. G. Arnaut, A. P. Monkman, I. Hamblett, and S. Navaratnam, J. Chem. Phys. **115**, 9601 (2001).
[47] V. R. Nikitenko, D. Hertel, and H. Bässler, Chem. Phys. Lett. **348**, 89 (2001).
[48] B. Movaghar, M. Grünewald, B. Ries, H. Bässler, and D. Würtz, Phys. Rev. B **33**, 5545 (1986).
[49] H. Bässler, Phys. Status Solidi B **175**, 15 (1993).
[50] M. Scheidler, B. Cleve, H. Bässler, and P. Thomas, Chem. Phys. Lett. **225**, 431 (1994).